scientific reports

Check for updates

OPEN

First-principle study on the stability of Cd passivates in soil

Jianglong Shen[1,2,3,4]✉, Juan Li[1,2,3,4], Zhongan Mao[1,2,3,4] & Yang Zhang[1,2,3,4]

The stable existence of heavy metals in soil under natural conditions is the core issue in heavy metal pollution solidification and remediation technology. However, the existing research is limited to soil passivation tests of different materials or biochar adsorption tests and cannot reveal the internal mechanism of functional groups of different compounds in soil passivation. This paper takes the common heavy metal ion Cd^{2+} as an example to analyze the stability of the combination of heavy metal ions and common ion groups in soil. The stability and existing form of Cd are analyzed by using first-principle calculations, and the free energy, band structure, and partial density of states of $CdCO_3$, $CdSO_4$, $CdCl_2$, and $CdSiO_3$ are computed. The stability of Cd binding to common anions in soil is determined. Results show the descending order of structural stability of cadmium compounds is $CdSiO_3$, $CdSO_4$, $CdCO_3$, and $CdCl_2$. SO_4^{2-} and SiO_3^{2-} can be used as preferred functional groups for cadmium pollution passivation. Anhydrous sodium sulfate and sodium silicate are promising passivators.

With the development of society, the degree of industrialization is increasing. The industrial waste generated by industrial production activities as the source of heavy metal pollution is usually not properly treated[1–3]. In the long run, the pollution sources are increasing, and more heavy metals enter the soil through various ways and then continue to accumulate in the soil to form pollution[4–8]. Soil plays a fundamental role in food safety, and the adverse effects of contaminants like heavy metal (loid)s on crop quality have threatened human health[9–17]. The theoretical optimal scheme for remediation of agricultural nonpoint source heavy metal pollution is to add amendments in contaminated soil, change the heavy metal elements from bioavailable state to residual state, limit the migration of heavy metal ions, and achieve in-situ remediation. To improve research and development, knowing the physical and chemical properties of heavy metal pollutants is of great importance. Understanding the solidification, adsorption, and precipitation of such pollutant heavy metals under normal temperature and pressure is the key research content. At this stage, the nature of soil Cd pollution is mainly determined through experiments, such as infrared scanning, Raman laser spectroscopy, and X-ray diffraction[18–21]. Phosphoric acid and sulfur compounds can be used as stabilizers of cadmium. However, the experimental observation results cannot explain the theoretical problems, and one observation cannot ensure that it conforms to the laws of physics and chemistry. In addition, the precipitation conditions of cadmium-containing compounds are different from the natural state of soil chemistry[22,23]. The stability of cadmium-containing compounds cannot be fundamentally solved by traditional chemical theories. The above problems can be solved by using quantum geochemical tools to calculate the stability of the combination of CO_3^{2-}, SO_4^{2-}, Cl^-, SiO_3^{2-} plasma, and Cd^{2+}. At present, reports on the theoretical study of the energy stability of various cadmium compounds are few.

First-principle calculation has been widely used in many scientific research directions, such as the simulation of unknown material properties in materials science, such as the design and synthesis of functional photoelectric materials by calculating the photoelectric properties of materials. In geology, it is used to simulate the structure and composition[10,24–28]. In thermodynamics, the simulated formation and configuration of minerals are studied. The research on passivating agent for in-situ remediation of heavy metal pollution is still in the research stage of what kind of substance is used as passivating agent and its passivating effect[29]. Few studies have applied the first-principle calculation in the calculation of heavy metal passivation. Common acid ions, such as chloride ion, carbonate ion, silicate ion, and sulfate ion, are introduced into the calculation of cadmium containing system by using first-principle calculation. In this way, the stability of the combination of functional groups and Cd^{2+} can be better understood to design more suitable soil remediation passivators.

[1]Key Laboratory of Degraded and Unused Land Consolidation Engineering, Ministry of Natural Resources, Xi'an 710075, China. [2]Institute of Land Engineering and Technology, Shaanxi Provincial Land Engineering Construction Group Co., Ltd., Xi'an 710075, China. [3]Shaanxi Provincial Land Engineering Construction Group Co., Ltd., Xi'an 710075, China. [4]Shaanxi Provincial Land Consolidation Engineering Technology Research Center, Xi'an 710075, China. ✉email: shen@edu.email.cn

Calculation principle and method

According to the principle of interaction between nucleus and electron and its basic motion law, the principle of quantum mechanics is applied, and the Schrodinger equation is solved directly after some approximate processing algorithm, called first-principle calculations. First-principle calculations include two major categories, Hartree–Fock self-consistent field calculations based on ab initio and density functional theory (DFT) calculations[30]. The first-principle calculation using Vienna Ab initio Simulation Package (VASP)[31,32] software in this paper is based on DFT. At normal temperature and pressure, Gibbs free energy plays a decisive role in material stability. The Gibbs free energy calculation formula is G = H − TS, H = U + PV, where G is the Gibbs free energy, H is the enthalpy, T is the Fahrenheit temperature, S is the entropy, U is the internal energy of the system, P is the pressure, and V is the volume. H, T, and S are state functions. G is a state function, representing the properties of a particular state. Given that the entropy value has difficulty determining the exact value, the Fahrenheit temperature is set as absolute zero, the crystal structure from absolute zero to normal temperature and pressure has not been deformed, and the properties are consistent. Hence, extrapolating the properties calculated from the free energy under absolute zero to those under normal temperature and pressure is reasonable. Under stable conditions, substances react in the direction of lower Gibbs free energy to form substances with lower Gibbs free energy value, which can be used to judge the stability and reaction direction of heavy metal compounds[33,34].

In this paper, crystal coefficient files in the crystal library are needed to establish the corresponding crystals, process them with CATSEP in Materials Studio, and then place them into VASP package for first-principle calculation. The projection method is projection augmented wave method, and PAW_PBE is selected as a pseudopotential of projected augmented wave, which functions as PBE exchange key energy functional. The electron orbit of cadmium is corrected by GGA + U treatment of 3d electron orbit and then calculated accordingly. Parameters in the calculation are set as follows: PREC = accurate, and EDIFF = 1.E−05 conversion unit is set as eV, that is, the convergence point energy limit is 10^{-5}, and the corresponding convergence energy limit between atoms is 10^{-2} eV/nm. In the optimization, the optimized NSW = 200 is selected, that is, the number of motion steps in the nucleus is 200, and the subsequent self-consistent motion in the nucleus keeps the nucleus stationary, that is, NSW = 0. The calculation of each system is carried out after the convergence test, in which the truncation energy and the parameter setting of Brillouin zone location point (K point) adopt the corresponding value according to the different calculation systems, and the selection of K point adopts the Monkhorst Pack method. The plane wave truncation energy is optimized by using the equal difference number sequence of 200, 250, 300, 350, 400, 450, 500, 550, and 600 eV to determine that 500 eV is the most appropriate truncation energy because the structural optimization part and the energy calculation part have different requirements for accuracy.

The expansion width of heavy metal cadmium in the calculation parameter setting is selected as SIGMA = 0.05. In the K-point selection, considering accuracy and calculation cost, the optimization should be as large as possible when the calculation accuracy allows. When calculating the density of states, the K-point value should be relatively reduced. The highly symmetric K-point distribution is adopted in the calculation of energy band.

Results and discussion

Selection and optimization of crystal structure. After comprehensively considering factors such as the difficulty of obtaining cadmium compound groups, purity, and process level, the type of cadmium-containing crystals used for calculation was selected, which provides reference for the selection of passivating agents in the later stage. The anion group is chloride ion, carbonate, silicate, and sulfate, and the chemical formulas are $CdCl_2$, $CdCO_3$, $CdSiO_3$, and $CdSO_4$, respectively. The corresponding crystal structures of the above compounds were obtained from the Crystallography Open Database in Fig. 1.

Table 1 shows the cell structure parameters of four cadmium compounds after optimization. The unit cell parameters optimized by VASP calculation are very close to the ideal experimental values, and the change ratio is within 0.2%, which further indicates the theoretical calculation by VASP is the same as the experimental results under ideal conditions. The deviation between the bond length and bond angle in the unit cell and the ideal experimental value after VASP optimization is within 0.8%, which indicates VASP does not substantially change the original structure of the unit cell when calculating these units, and cadmium and corresponding ionic groups in the unit cell can maintain the original physical and chemical properties.

Free energy. The energy system of $CdCl_2$, $CdCO_3$, $CdSiO_3$, and $CdSO_4$ at room temperature and pressure is calculated by the first-principle software VASP, as shown in Table 2. The ascending order of Gibbs free energy of the four cadmium containing systems from is $CdSiO_3$, $CdSO_4$, $CdCO_3$, and $CdCl_2$. The relative stability of these systems is inversely related to their corresponding Gibbs free energy ordering. The predicted descending order of the relative structural stability of four simple cadmium compounds is $CdSiO_3$, $CdSO_4$, $CdCO_3$, and $CdCl_2$.

Band structure and partial density of states. By calculating the band values of the above systems, the band structures are derived, and more detailed structural information of these systems is obtained to understand the electrical properties, crystal configurations, and chemical bond types of these systems deeply, and determine the functional groups polluted by cadmium passivation better[35–40]. Figure 2 shows the Fermi energy level (Efermi) is taken as the energy zero. The band gap widths of $CdCl_2$, $CdCO_3$, $CdSiO_3$, and $CdSO_4$ are 3.53, 2.98, 1.32, and 3.09 eV, respectively. These four systems are semiconductors, but their conductivity is weak. Figure 2 shows the top of the valence band of the four systems, $CdCl_2$, $CdCO_3$, $CdSiO_3$, and $CdSO_4$, is closer to its corresponding Fermi energy level in the system (the position of 0 eV in the figure), and the conduction band of these systems is more volatile. These systems are p-type semiconductors[41–44]. In addition, the crystal structure of these systems is not filled with electrons, and attracting electrons to fill the crystal holes is easier when the properties change. The energy band of this series of systems is narrow due to the relatively dense electrons in the

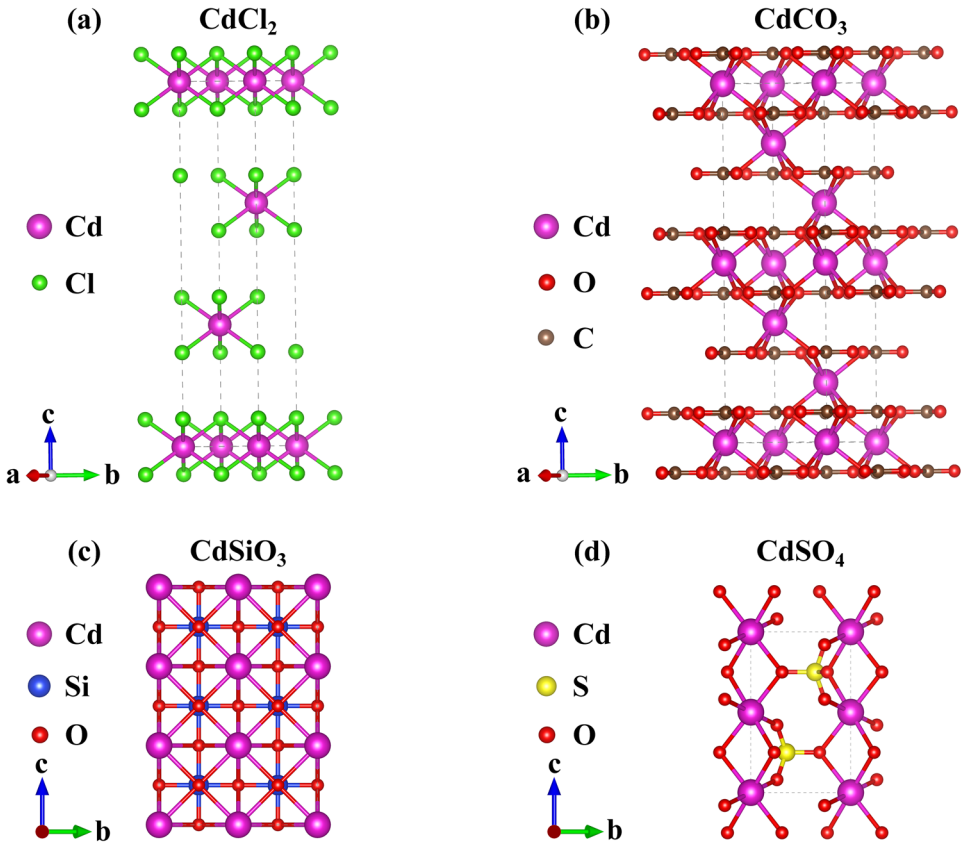

Figure 1. Cell structure of $CdCl_2$, $CdCO_3$, $CdSiO_3$, and $CdSO_4$.

Model	Lattice constant (Å)			Shaft angle			Volume (Å^3)
	a	b	c	α	β	γ	
$CdCl_2$	3.9259	3.9259	18.9468	90	90	120	252.8943
$CdCO_3$	4.9204	4.9204	16.298	90	90	120	341.7164
$CdSiO_3$	7.2398	7.2398	10.8598	90	90	90	569.2174
$CdSO_4$	4.9978	4.9978	7.3134	90	90	90	166.0376

Table 1. Cell parameters of $CdCl_2$, $CdCO_3$, $CdSiO_3$, and $CdSO_4$.

System	Fermi level (eV)	Free energy (J/g atom)
$CdCl_2$	−0.368	−7.8643124
$CdCO_3$	1.4326	−63.875465
$CdSiO_3$	5.4327	387.048856
$CdSO_4$	1.7624	−67.875434

Table 2. Energy parameters of $CdCl_2$, $CdCO_3$, $CdSiO_3$ and $CdSO_4$.

energy band position in the crystal structure, which is caused by the overlap of some hybrid orbitals. It has more effective electrons and higher relative mass. These systems fluctuate greatly in the direction from the center of the Brillouin zone to the center of the quadrilateral surface, so more attention should be paid to the selection and manufacture of passivation that change their structural properties.

Partial density of states (PDOS) is another way to present the crystal structure. The combination of PDOS and energy band structure map in Fig. 2 can better reflect its crystal structure properties. The size of PDOS can replicate the strong degree of the combination of cations and anions in the system, thus inferring the relative stability order of these systems. In addition, PDOS can directly reflect the influence of different anion groups on the electronic density of the whole system[45–50]. Figure 2 shows the PDOS of $CdCl_2$, $CdCO_3$, $CdSiO_3$, and $CdSO_4$

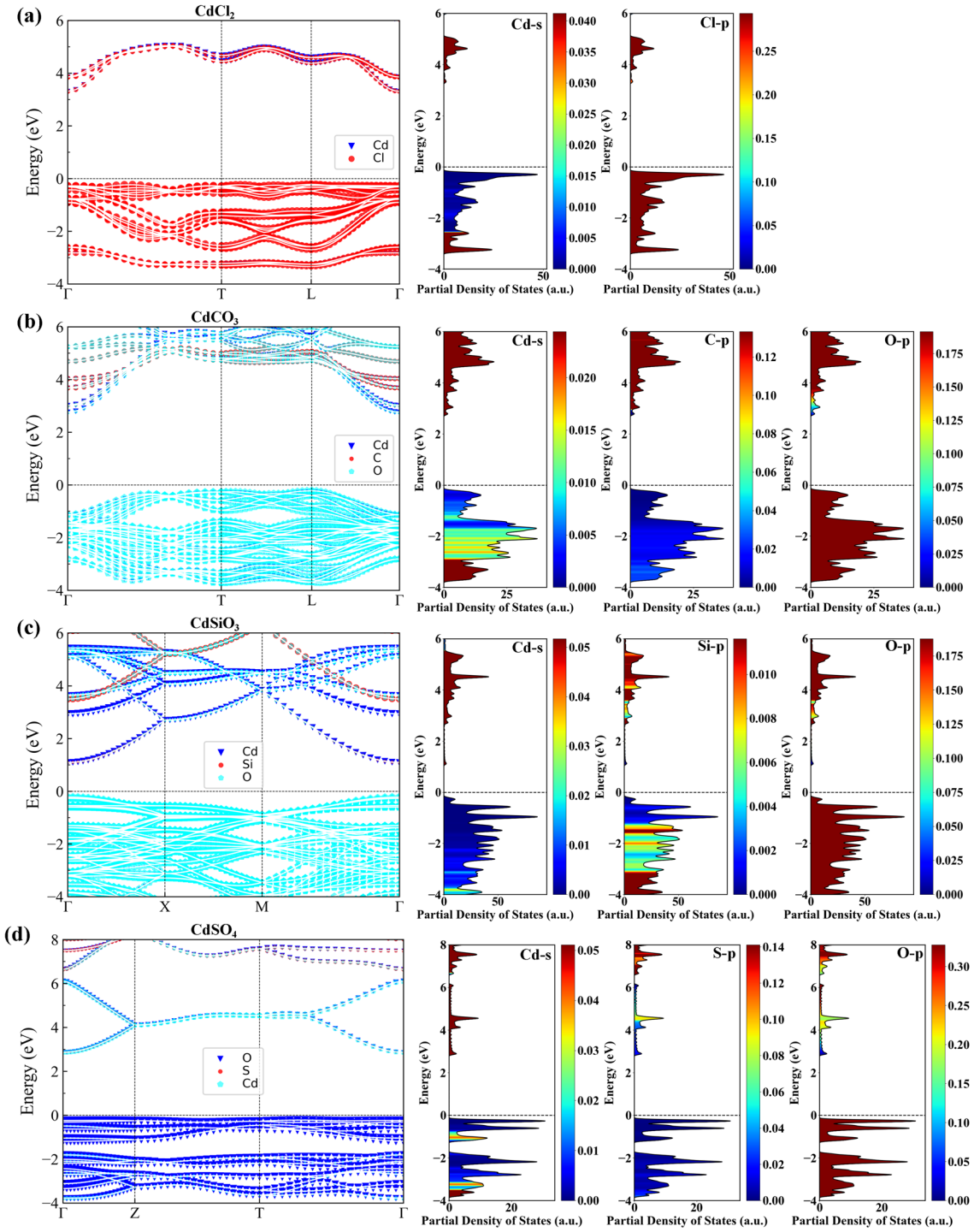

Figure 2. Band structure (left) and partial density of states (PDOS) (right) of four systems: (**a**) $CdCl_2$, (**b**) $CdCO_3$, (**c**) $CdSiO_3$, and (**d**) $CdSO_4$ (Note: 0 eV represents its corresponding Fermi energy level, where the abscissa Γ Gamma point, the center of Brillouin zone).

systems have local sharpening peaks in the conduction band and the valence band. The electrons in these areas are denser than those in other locations in the crystal, and the presented aggregation rule is mutually corroborated by the narrower energy band in the corresponding location displayed in the energy band structure[51]. The dispersion of the valence band in the $CdSO_4$ system is higher than that of $CdSiO_3$, $CdCO_3$, and $CdCl_2$, indicating the binding force of Cd^{2+} and SO_4^{2-} is stronger.

In the $CdCl_2$ system, the contribution of the s orbital of Cd to the system is mainly reflected in the bottom of the conduction band, and the main contribution of the p orbital of Cl to the system is reflected in the valence band. In the $CdCO_3$ system, the main contribution of the s orbit of Cd to the system is reflected in the bottom of the conduction band, the main contribution of the p orbit of C to the system is reflected in the bottom of the

conduction band, and the main contribution of the p orbit of O to the system is reflected in the valence band. In the $CdSiO_3$ system, the contribution of the s orbital of Cd to the system is mainly reflected in the bottom of the conduction band, the contribution of the p orbital of Si to the system is mainly reflected in the conduction band, and the contribution of the p orbital of O to the system is reflected in the valence band. In the $CdSO_4$ system, the contribution of the s orbital of Cd to the system is mainly reflected in the conduction band, and the contribution of the p orbital of O to the system is mainly reflected in the valence band. According to the calculated original PDOS values, the electron density in these four systems is high in the s-orbital contribution rate and low in the p-orbital contribution rate. Table 3 describes the density of state percentage and the density of state ratio of the anion and cation groups of various compounds containing cadmium in the system. Among the selected series, SO_4^{2-} accounts for the highest proportion of anions in the compound system containing cadmium, which plays a decisive role in stability, and $SiO3^{2-}$ is also better than Cl^-. Thus, SO_4^{2-} and SiO_3^{2-} may be the preferred functional groups for cadmium ion passivation.

Test application. According to first-principle calculation, the best functional groups for controlling cadmium pollution were obtained. When selecting passivating agent in practical application, the mature process and easy release of SiO_3^{2-} and SO_4^{2-} should be considered first. Therefore, anhydrous sodium sulfate ($NaSO_4$) and sodium silicate ($Na_2SiO_3{\cdot}9H_2O$) with mature technology and easy to release cation exchange and anionic functional groups should be prioritized as passivating agents. Although the production of these samples is mature, they face the problem of high price when used in large quantities, so finding low-cost, efficient substitutes is necessary. The improvement method was to select low-cost industrial byproduct desulfurized gypsum (the main component is $CaSO_4{\cdot}2H_2O$, the same as natural gypsum, content, 93%) as passivating agent. To verify the control effect of the above-mentioned three passivating agents on cadmium pollution, the natural soil of Guanzhong was used as raw material to prepare cadmium-contaminated soil by adding compounds that can release Cd^{2+}. Cd(II) standard liquid, sodium dihydrogen phosphate (NaH_2PO_4), sodium sulfate (Na_2SO_4), desulfuration gypsum ($CaSO_4{\cdot}2H_2O$, content ≥ 93%), and diethylenetriaminepentaacetic acid were purchased from Shanghai Chemical Reagents Company (China), Cd(II) standard liquid was guaranteed reagent, and others were analytical reagents. Thrice the cadmium pollution control value (500 mg/kg) of $CdCl_2$ was added to the pollution-free soil. $CdCl_2$ was dissolved in water and evenly poured into the pollution-free original soil. To shorten the duration of the experiment, the soil added with pollutants was placed in a constant temperature and humidity incubator for aging treatment, and the aging duration was 40 days. The initial mass fraction of Cd^{2+} in the self-made contaminated soil was 1432.5 mg/kg. Sodium dihydrogen phosphate, anhydrous sodium sulfate, and desulfurization gypsum (93% purity) of 2% of the soil mass to be treated were added to the self-made contaminated soil. The soil was stirred once a day, and the mass fraction of available cadmium in soil was measured after 3, 7, and 15 days of treatment. The measurement results are shown in Table 4.

Table 4 shows the three passivators have remarkable control effects on Cd^{2+} in contaminated soil. In 15 days, the mass fraction of available cadmium can be reduced by 28.56–39.23%. Among them, anhydrous sodium sulfate has the best effect, which verifies that SO_4^{2-} and SiO_3^{2-} can be used as effective functional groups to control cadmium pollution.

Conclusion and discussion

The control of soil Cd pollution has always been a hot issue in scientific research, and soil health is related to the lifeblood of human development[52,53]. Much of the existing research had experimentally focused on the remediation of contaminated soil[54–57]. These methods consider the characteristics of high activity and large specific surface area of biochar, and adsorb heavy metal elements in soil, but the characteristics of Cd compounds themselves were not fully studied. In this paper, first-principle calculations are used to study the potential of different passivators in soil for cadmium. This approach provides a new perspective on the study of environmental

System	Anion group ratio (%)	Cation group ratio (%)	Anion/cation
$CdCl_2$	20.43	27.14	0.75
$CdCO_3$	47.83	27.52	1.73
$CdSiO_3$	48.31	26.98	1.79
$CdSO_4$	51.32	19.38	2.64

Table 3. Proportion of groups in $CdCl_2$, $CdCO_3$, $CdSiO_3$ and $CdSO_4$.

Time/d	NaH_2PO_4	Na_2SO_4	$CaSO_4{\cdot}2H_2O$
0	1475.2	1475.2	1475.2
3	1148.15	1187.3	1289.54
7	1043.25	1098.73	1187.49
15	896.56	935.87	1053.76

Table 4. Active mass fraction of cadmium after passivating agent addition.

pollution of heavy metals. The geometry, electronic structure, state density, charge transfer, and energy conversion of different cadmium compound crystals are analyzed, and the internal mechanism of various cadmium compounds in passivation is clarified. Experimental studies show this method is feasible.

According to first-principle calculation, the Gibbs free energy of the four cadmium-containing systems is in the ascending order of $CdSiO_3$, $CdSO_4$, $CdCO_3$, and $CdCl_2$, and the structural stability of cadmium compounds is in the descending order of $CdSiO_3$, $CdSO_4$, $CdCO_3$, and $CdCl_2$.

Based on the discussion of energy band structure and PDOS, $CdCO_3$, $CdSO_4$, $CdCl_2$, and $CdSiO_3$ are all p-type semiconductors. The crystal structures of these systems are not filled with electrons, and they are more likely to attract electrons to fill the crystal cavities when the properties change. However, the n-type semiconductor of $CdSiO_3$ system shows metallicity. The electrons in the lattice are more active and can migrate and conduct in the lattice. Losing the electrons in the crystal is easier when the properties change.

In the cadmium-containing system, CO_3^{2-}, SO_4^{2-}, Cl^-, SiO_3^{2-}, and other ionic groups are analyzed, and SO_4^{2-} and SiO_3^{2-} can be used as the preferred functional groups for cadmium-contaminated passivation. Anhydrous sodium sulfate and sodium silicate are effective passivating agents. If cost and large area promotion are considered, low-cost desulfurization gypsum is preferred.

Data availability

The datasets generated and analysed during the current study are not publicly available due this experiment was a collaborative effort, the trial data does not belong to me alone but are available from the corresponding author on reasonable request.

Received: 26 January 2023; Accepted: 13 March 2023
Published online: 14 March 2023

References

1. Lin, Z. *et al.* Ranking of mechanisms governing the phytoavailability of cadmium in agricultural soils using a mechanistic model. *Plant Soil* **399**, 89–107 (2016).
2. Chen, H. Y. *et al.* Contamination features and health risk of soil heavy metals in China. *Sci. Total Environ.* **512**, 143–153 (2015).
3. Li, M. Y. *et al.* Human health risk assessment of heavy metals in food: A review. *J. Fujian Agric. For. Univ. (Natural Science Edition)* **50**, 1–9 (2021).
4. Diami, S. M., Kusin, F. M. & Madzin, Z. Potential ecological and human health risks of heavy metals in surface soils associated with iron ore mining in Pahang, Malaysia. *Environ. Sci. Pollut. Res.* **23**, 21086–21097 (2016).
5. Chaudhry, S. A., Khan, T. A. & Ali, I. Adsorptive removal of Pb(II) and Zn(II) from water onto manganese oxide-coated sand: Isotherm, thermodynamic and kinetic studies. *Egypt. J. Basic Appl. Sci.* **3**, 287–300 (2016).
6. Ahmad, M. *et al.* Biochar induced changes in soilproperties affected immobilization/mobilization of metals/metal loids in-contaminated soils. *J. Soils Sediments* **17**, 717–730 (2017).
7. Gu, Q. B. *et al.* Application of ecogeochemical prediction model to safely exploit seleniferous soil. *Ecotoxicol. Environ. Saf.* **177**, 133–139 (2019).
8. Jiang, X. L. *et al.* Distribution, source identification, and ecological risk assessment of heavy metals in wetland soils of a river-reservoir system. *Environ. Sci. Pollut. Res.* **24**, 436–444 (2017).
9. Briffa, J., Sinagra, E. & Blundell, R. Heavy metal pollution in the environment and their toxicological effects on humans. *Heliyon* **6**, e04691 (2020).
10. Qin, G. *et al.* Soil heavy metal pollution and food safety in China: Effects, sources and removing technology. *Chemosphere* **267**, 129205 (2021).
11. Vareda, J. P., Valente, A. J. M. & Durães, L. Assessment of heavy metal pollution from anthropogenic activities and remediation strategies: A review. *J. Environ. Manag.* **246**, 101–118 (2019).
12. Wu, Y. *et al.* Review of soil heavy metal pollution in China: Spatial distribution, primary sources, and remediation alternatives. *Resour. Conserv. Recycl.* **181**, 106261 (2022).
13. Fei, X. *et al.* Source analysis and source-oriented risk assessment of heavy metal pollution in agricultural soils of different cultivated land qualities. *J. Clean. Prod.* **341**, 130942 (2022).
14. Xie, N. *et al.* Assessment of the variation of heavy metal pollutants in soil and crop plants through field and laboratory tests. *Sci. Total Environ.* **811**, 152343 (2022).
15. Han, I. *et al.* Heavy metal pollution of soils and risk assessment in Houston, Texas following Hurricane Harvey. *Environ. Pollut.* **296**, 118717 (2022).
16. Zhao, H. *et al.* Comprehensive assessment of harmful heavy metals in contaminated soil in order to score pollution level. *Sci. Rep.* **12**, 3552 (2022).
17. Iordache, A. M. *et al.* Accumulation and ecotoxicological risk assessment of heavy metals in surface sediments of the Olt River, Romania. *Sci. Rep.* **12**(1), 880 (2022).
18. Eziz, M., Hayrat, A. & Yang, X. Y. Comparison and analysis of estimation methods for heavy metal pollution of farmland soils. *J. Resour. Ecol.* **11**, 435–442 (2020).
19. Tang, X. *et al.* Review of remediation practices regarding cadmium-enriched farmland soil with particular reference to China. *J. Environ. Manag.* **181**, 646–662 (2016).
20. Ruby, M. V. & Lowney, Y. W. Selective soil particle adherence to hands: implications for understanding oral exposure to soil contaminants. *Environ. Sci. Technol.* **46**, 12759–12771 (2012).
21. Lim, J. *et al.* Effects of natural and cal▪cined poultry waste on Cd, Pb and As mobility in contaminated soil. *Environ. Earth Sci.* **69**, 11–20 (2013).
22. Zhong, Q. Y. *et al.* Addition on uptake of heavy metals and arsenic in paddy fields. *Acta Ecol. Sin.* **35**, 1242–1248 (2015).
23. Wang, J. J. *et al.* Research on the risk level-based technology integration for the remediation of heavy metals polluted farm land. *J. Agro Environ. Sci.* **38**, 249–256 (2019).
24. Li, Y. *et al.* Effect of amendments on heavy metal availability in soil and uptake of heavy metals by soybeans. *J. Saf. Environ.* **19**, 1737–1744 (2019).
25. Han, Y. *et al.* Heavy metals in soil contaminated through e-waste processing activities in a recycling area: Implications for risk management. *Process Saf. Environ. Prot.* **125**, 189–196 (2019).
26. Gao, Y., He, J. H. & Guo, H. Z. The optimal tuning of electronic structure, magnetic, and optical properties of (Fe, V+ VO/VSn) co-doped SnO_2 via first-principles calculations. *J. Chem. Phys.* **157**, 224102 (2022).

27. Gao, Y., Hou, Y. Q. & Liu, Q. L. First-principles study on the electronic structures and magneto-optical properties of $Fe^{2+/3+}$ doped SnO_2. *Solid State Commun.* **305**, 113764 (2020).
28. Gao, Y., He, J. H. & Guo, H. Z. Effect of co-doping and defects on electronic, magnetic, and optical properties in SnO_2: A first-principles study. *Phys. B* **639**, 413924 (2022).
29. Li, S. W. *et al.* Assessment of cadmium bioaccessibility to predict its bioavailability in contaminated soils. *Environ. Int.* **94**, 600–606 (2016).
30. Tian, H. Q. *et al.* Effects of soil properties and land use type son the bioaccessibility of Cd, Pb, Cr, and Cu in Dongguan City, China. *Bull. Environ. Contam. Toxicol.* **104**, 64–70 (2020).
31. Kresse, G. & Hafner, J. Ab initio molecular dynamics for liquid metals. *Phys. Rev. B* **47**, 13115–13118 (1993).
32. Kresse, G. & Furthmüller, J. Efficiency of ab-initio total energy calculations for metals and semiconductors using a plane-wave basis set. *Comput. Mater. Sci.* **6**, 15–50 (1996).
33. Zhang, Z. *et al.* Arc melting: a novel method to prepare homogeneous solid solutions of transition metal carbides (Zr, Ta, Hf). *Ceram. Int.* **45**, 9316–9319 (2019).
34. Sarker, P. *et al.* High-entropy high-hardness metal carbides discovered by entropy descriptors. *Nat. Commun.* **9**, 4980 (2018).
35. Lyu, C. *et al.* Microbial induced carbonate precipitation cntributes to the fates of Cd and Se in Cd-contaminated seleniferous soils. *J. Hazard. Mater.* **423**, 126977 (2022).
36. Zhang, Y. *et al.* Simultaneous scavenging of Cd (II) and Pb (II) from water by sulfide-modified magnetic pinecone-derived hydrochar. *J. Clean. Prod.* **341**, 130758 (2022).
37. Tang, B. *et al.* Effect of biochar on immobilization remediation of Cd▪contaminated soil and environmental quality. *Environ. Res.* **204**, 111840 (2022).
38. Feng, Z. *et al.* $KHCO_3$ activated biochar supporting MgO for Pb (II) and Cd (II) adsorption from water: Experimental study and DFT calculation analysis. *J. Hazard. Mater.* **426**, 128059 (2022).
39. Gao, B. *et al.* Biogeochemical Fe (II) generators as a new strategy for limiting Cd uptake by rice and its implication for agricultural sustainability. *Sci. Total Environ.* **820**, 153306 (2022).
40. Qutub, N. *et al.* Enhanced photocatalytic degradation of Acid Blue dye using CdS/TiO_2 nanocomposite. *Sci. Rep.* **12**, 5759 (2022).
41. Mandal, A. Tuning p-type to n-type semiconductor nature by charge transfer cocrystallization: Effect of transfer integral vs. reorganization energy. *CrystEngComm* **24**, 2072–2080 (2022).
42. Kim, T. & Jeong, J. K. Recent progress and perspectives of field-effect transistors based on p-type oxide semiconductors. *Phys. Status Solidi (RRL) Rapid Res. Lett.* **16**, 2100394 (2022).
43. Maksymych, V., Ivashchyshyn, F., Całus, D. *et al.* Electrical properties of clathrate formed on the basis of a p-type semiconductor with 2D guest positions filled with ferroelectric and propolis. *Appl. Nanosci.* 1–8(2022).
44. Li, Y. *et al.* Improved thermal stability and enhanced thermoelectric properties of p-type $BaCu_2Te_2$ by doping of Cl. *ACS Appl. Mater. Interfaces* **14**, 5634–5642 (2022).
45. Guo, Z. *et al.* Electrocatalytic dinitrogen reduction reaction on silicon carbide: A density functional theory study. *Phys. Chem. Chem. Phys.* **22**, 21761–21767 (2020).
46. Yang, J. *et al.* Density functional theory study on the effect of sodium on the adsorption of NO on a char surface. *Energy Fuels* **34**, 8726–8731 (2020).
47. Zhou, Q. *et al.* Insight into the elemental mercury immobilization mechanism with carbon and sulfur over the mackinawite (FeS) surface via density functional theory. *Chem. Eng. J.* **450**, 137934 (2022).
48. Sangolkar, A. A. & Pawar, R. Structure, stability, properties, and application of atomically thin coinage metal flatland in graphene pore: A density functional theory calculation. *Phys. Status Solidi B* **259**, 2100489 (2022).
49. Miao, Y. *et al.* Adsorption of hydrated Al^{3+} on the kaolinite (001) surface: A density functional theory study. *Appl. Clay Sci.* **223**, 106498 (2022).
50. Wang, X. *et al.* Density functional theory study of Pd, Pt, and Au modified GeSe for adsorption and sensing of dissolved gases in transformer oil. *Surf. Interfaces* **31**, 101994 (2022).
51. Pham, T. N. *et al.* Density functional theory study of $NO–H_2O$ coadsorption on Cu (111). *Phys. Rev. Mater.* **6**, 075801 (2022).
52. Khan, S. *et al.* Global soil pollution by toxic elements: Current status and future perspectives on the risk assessment and remediation strategies–A review. *J. Hazard. Mater.* **417**, 126039 (2021).
53. Song, S., Zuo, J. & Chang, Q. Effects of heavy metal pollution in soil of coal gangue area on germination and seedlings of typical remediation plants. *Sustainability* **15**, 3359 (2023).
54. Jing, F. *et al.* Biochar effects on soil chemical properties and mobilization of cadmium (Cd) and lead (Pb) in paddy soil. *Soil Use Manag.* **36**, 320–327 (2020).
55. Albert, H. A. *et al.* Influence of biochar and soil properties on soil and plant tissue concentrations of Cd and Pb: A meta-analysis. *Sci. Total Environ.* **755**, 142582 (2021).
56. Naeem, I. *et al.* Prospective usage of magnesium potassium phosphate cement combined with *Bougainvillea alba* derived biochar to reduce Pb bioavailability in soil and its uptake by *Spinacia oleracea* L. *Ecotoxicol. Environ. Saf.* **208**, 111723 (2021).
57. Song, P. *et al.* Remediation mechanism of Cu, Zn, As, Cd, and Pb contaminated soil by biochar-supported nanoscale zero-valent iron and its impact on soil enzyme activity. *J. Clean. Prod.* **378**, 134510 (2022).

Acknowledgements

This research was funded by the Natural Science Basic Research Program of Shaanxi Province(2023-JC-QN-0360), Shaanxi Provincial Technical Innovation Guidance Project(S2021-YD-CGZH-0054), Internal scientific research project of Shaanxi Land Engineering Construction Group Co., Ltd(DJNY2022-25), Shaanxi Province Innovation Capability Support Plan Project(2021PT-053), Shaanxi Province Innovative Talents Program-Youth Science and Technology Rising Star Project (2021KJXX-88), and Technology innovation Center for Land Engineering and Human Settlements, Shaanxi Land Engineering Construction Group Co., Ltd. and Xi'an Jiaotong University (2021WHZ0093).

Author contributions

The manuscript was reviewed and approved for publication by all authors. J.L.S. conceived and designed the experiments. J.L. performed the experiments, analyzed the data, drew the figures and wrote the paper. Z.A.M. and Y.Z. revised the paper.

Competing interests

The authors declare no competing interests.

Additional information

Correspondence and requests for materials should be addressed to J.S.

Reprints and permissions information is available at www.nature.com/reprints.

Publisher's note Springer Nature remains neutral with regard to jurisdictional claims in published maps and institutional affiliations.